LHCB-MUON 2003-040
27th May 2003

Aging test of a prototype of quadrigap MWPC for the region 3 of the LHCb muon system

M. Anelli, P. Campana, C. Forti, R. Rosellini, M. Santoni, A. Sciubba
Laboratori Nazionali dell'INFN, Frascati, Italy

S. Baccaro
ENEA-FIS/ION, C.R. Casaccia, 00060 S.Maria di Galeria (Roma), Italy

Abstract

We present the results of an aging test on a quadrigap prototype of MPWC of the LHCb muon system. The test was carried out with the Co^{60} source of the Calliope gamma facility at ENEA-Casaccia Research Center, near Rome. The main goal of this short test was to check the feasibility and the optimal conditions for a longer test. We monitored the current in the test chamber and in a similar reference chamber, recording the room temperature and the atmospheric pressure. Over a test duration of $\sim 90\ hours$, we integrated $\sim 50\ mC/cm$ of wire, without any appreciable deterioration of the detector.

Contents

1 Introduction

In this note we report the results of an aging test of a MWPC, assembled in Frascati Laboratories of INFN, prepared for the muon system of the LHCb experiment. A similar prototype (but with two gaps instead of 4) has already been tested at CERN beam [1].

The main goal of this short test is to check the feasibility of a longer test (about one month is required for an aging of 10 equivalent LHC years in the M2R1 region) and to understand the main problems arising.

We monitored the current in two quadrigap chambers: a test chamber and a monitor one (the latter exposed to a dose rate ~ 17 times smaller). Both chambers are identical to the prototype described in detail in [1] and in [2]. Here we just remind that each prototype is composed of four gaps, each with an anode wire plane (pitch $1.5\ mm$) at the center of the gap ($5\ mm$), a plane of cathode pads and a ground plane. Each gap has 134 W wires $\sim 25\ cm$ long and a sensitive area of $\sim 200 \times 251\ mm^2$, representing 1/6 of one final WPC for region M3R3.

In Section 2 we shortly describe the Calliope gamma facility where the test was carried out. In Section 3 we describe the experimental setup. Then, in Section4 we report the aging test results and the considerations for a longer test. In last Section, we draw the conclusions of the test.

2 The Calliope gamma facility

The test was carried out with the Co^{60} source of the Calliope gamma facility at ENEA-Casaccia Research Center, near Rome. Calliope γ plant is a pool-type irradiation facility equipped with a Co^{60} radioisotope source placed in a high-volume (7x6x3.9 m^3) and shielded cell [3].

The source is characterised by a cylindrical geometry with the Co^{60} pencils placed in the rack circumference . The emitted radiation consists of two photons with energy of 1.17 MeV and 1.32 MeV, mean energy being 1.25 MeV. The maximum licensed activity is $3.7\ 10^{15}$ Bq and the present activity is $9.05\ 10^{14}$ Bq (December 2002).

This plant offers the possibility to choose the dose rate for sample irradiation and the maximum dose rate (along the rack longitudinal axis) is 8240 Gy/h (December 2002). The storage water pool dimensions are 2x4.5x8 m^3 and two separate source emergency storage wells are positioned on the bottom of the pool. The irradiation protection shield is realized in baritic concrete (180 cm thickness).

To determine the irradiation dose rate, at the ”Calliope plant” three different dosimetric methods are available [4]: the Fricke absolute dosimetry (20-400 Gy), the alanine dosimetry (from

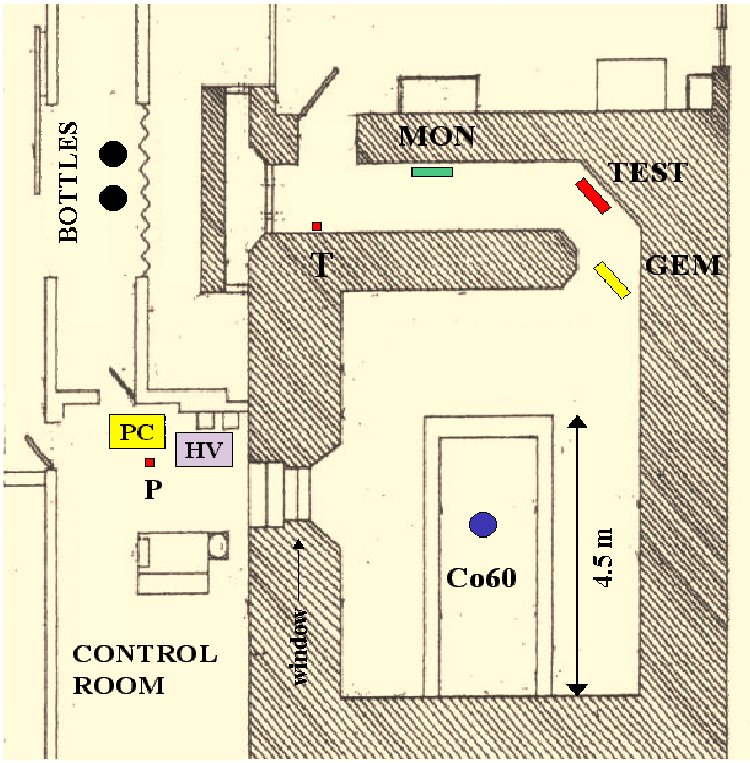

Figure 1: Map of the irradiation and control rooms. MON: MWPC monitor chamber. TEST: MWPC test chamber. GEM: GEM test chamber. T: temperature sensor. P: pressure sensor. BOTTLES: pre-mixed gas bottles for MWPC and GEM.

few Gy up to 500 kGy) and the Red Perspex dosimetry (5-50 kGy). Each irradiation tests is performed in charge particle equilibrium conditions and according to the various user demands (as the possibility to perform temperature controlled tests).

3 Setup for the aging test

We used two chambers with four gaps each: the "test" chamber was placed at about 4 meters from the source; the "monitor" chamber was far from the source, behind a concrete wall and with a lead sheet of 1.6 mm in front of it.

The gas mixture was Ar/CO_2/CF_4 with percentages 40/40/20. The two chambers were fluxed independently at a rate of $\sim$ 2 volumes/hour. We checked that the currents did not change at higher gas fluxes.

Using an electronic weather station Huger WM918, connected to a PC through the serial port, we monitored the temperature T in the irradiation room and the atmospheric pressure P.

A LabView program allows to read the 8 currents of the two quadrigap chambers and the information of the weather station and to record all data every 0.5 second.

During the test, also a GEM chamber was irradiated [5].

A map of the irradiation and control rooms is shown in Fig. 1.

Everytime an access to the room was needed, we first switched off all chambers, then put the source in the water pool. After the access, we first extracted the source from the pool, then we switched on again the chambers.

In Table 1 we summarize the main numbers of the test.

Figure 2: LEFT: The two racks supporting the MWPC test chamber (back) and the GEM (front) RIGHT: the monitor chamber mounted on a stool, placed behind a concrete wall.

In Fig. 2 the two racks supporting the GEM and the MWPC test chamber (left) and the MWPC monitor chamber (right) are shown.

In Fig. 3 we show the pool containing the source (left) and the test chamber (right).

Average gamma energy: $1.25\ MeV$	Dose rate for test chamber: $\sim 0.58\ Gy/hr$
Gas mixture: Ar 40% / CO_2 40% / CF_4 20%	Gas flux: $\sim$ 2 volumes/hour
Operating voltage: $3300\ V$	Average current in Test chamber: $\sim 500\mu A/gap$
Total wire length per gap$\sim 34m$	Current/cm of wire in Test chamber: $\sim 147nA/cm$
Atm. pressure range: $994 \div 1009\ mbar$	Temperature range: $288.6 \div 290.6$ K

Table 1: Summary of numbers caracterising the test setup.

4 Aging test results

4.1 Temperature and Atmospheric pressure

With a good approximation, the gas gain (and the current) are related to the high voltage (V) and the gas temperature (T) and pressure (P), according to the formula:

$$I = K \cdot e^{\alpha\ V\ T/P} \qquad (1)$$

During the test, we recorded the temperature T in the irradiation rooom and the atmospheric pressure P. Measurements were not available in the first day of test. We did not have sensors to measure directly the temperature and pressure of the gas mixture.

In Fig.4 (left) we show the temperature in the source room as function of time. It is not clear if the position of the peaks is due to the daily cycle: the time delays between the peaks are $\sim$ 16, $\sim$ 25 and $\sim$ 20 hours. The second peak corresponds to an access in the irradiation room, which may cause an increase in temperature (the sensor was near the door of the room).

Figure 3: LEFT: The pool containing the source. RIGHT: the test chamber mounted on the rack at $\sim 170\ cm$ from the floor.

In Fig.4 (right) we show the atmospheric pressure as function of time. After $\sim$ 45 hours, P starts increasing monotonically. We show below that this reflects on the currents.

The absolute values of T and P are known within $\pm$ 1 K for T and $\pm$ 7 mbar for P. We cannot state that T and P are precise estimates of the gas temperature and pressure inside the two chambers. Moreover, if the radiation heats the gas inside the chambers, the effect should be different for the two chambers. However, me must emphasize that the overall variation of T is $\sim 2/290 \sim 0.7\%$ and of P is $\sim 15/1000 \sim 1.5\%$.

4.2 Currents in monitor and test chambers

We recorded the currents of the 4 gaps of a monitor chamber, put behind a concrete wall and of the 4 gaps of the test chamber, exposed to a dose rate $\sim 0.58\ Gray/hr$. Both chambers were operating at HV=3300 V (except for some short measurements at other tension, to check detector current linearity). The values of the currents in the 4 gaps of the 2 chambers are reported in Table2 for several values of the high voltage. In Table3 we report the parameters of a quadratic fit of $ln(I)$ as function of V for the test gaps.

HV	A	B	C	D	A	B	C	D
0.	0.5	0.5	0.4	0.3	0.2	0.5	0.4	0.3
2000.	0.6	0.5	0.5	0.5	2.1	2.6	2.2	2.2
2700.	1.9	1.8	1.8	2.0	64.5	76.7	61.2	66.5
2850.	3.6	3.3	3.7	4.2	126.4	147.1	119.4	129.3
3000.	7.6	6.9	7.9	9.1	224.4	254.7	212.6	228.4
3150.	16.1	14.7	17.0	19.4	358.5	397.4	341.9	363.1
3300.	32.4	29.6	34.4	40.1	523.6	570.5	502.4	528.7

Table 2: Currents (in μA) as function of high voltage (V) in each gap of the (LEFT) monitor and (RIGHT) test chambers.

In Fig. 5 (LEFT) we show that the 4 gaps of the monitor chamber were operating in non-saturated condition. For an increase of 150 V in the high voltage, the gas gain approximately doubles. In the same figure (RIGHT) we show that the 4 gaps of the test chamber were operating

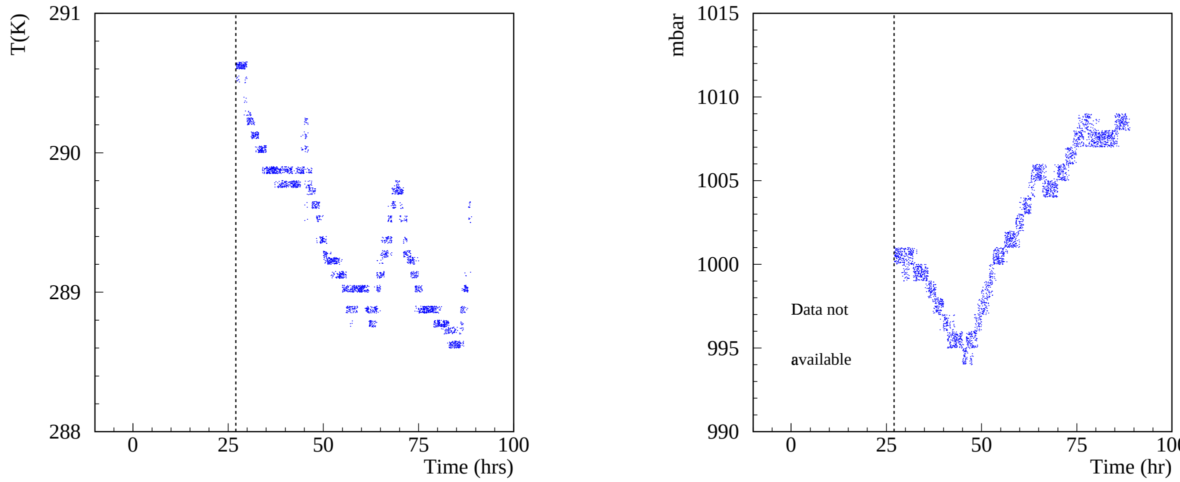

,

Figure 4: LEFT: Temperature in the source room as function of time. The cause of the peaks is not completely clear. RIGHT: Atmospheric pressure in the control room as function of time.

GAP	P_0	$P_1 \cdot 10^2$	$P_2 \cdot 10^6$	χ^2/NDF
A	-16.48	1.111	-1.275	0.65/3
B	-17.47	1.200	-1.446	0.41/3
C	-16.38	1.098	-1.248	0.59/3
D	-16.82	1.137	-1.324	0.55/3

Table 3: Parameters of the quadratic fit of $ln(I)$ as function of V for the test gaps.

in saturated condition. At 3300 V, the currents ($\sim$ 530 μA on average) are about a factor 2 below the expected value. At this dose rate, Log(I) vs. HV is linear up to $\sim$ 2850 V, where the current is $\sim$ 130 μA on average, about 1/4 respect to the value at 3300 V.

In Fig. 6 (LEFT) we show the currents of the 4 gaps of the monitor chamber as function of time. The maximum difference between the gaps is $\sim 30\%$. In the same figure (RIGHT) we show the currents in the test chamber. The smaller values are recorded either just after an access (full arrows) during which the chambers were switched off, or after some measurements at smaller HV (dashed arrow). The maximum difference between the gaps is $\sim 16\%$. As expected, all currents start decreasing when the pressure starts increasing (after $\sim$ 45 hours).

We remark that when the test chambers are switched on again after an access, several hours are needed to reach stable currents. This is better shown in Fig. 7 where we plot the currents just before and after an access.

The presence of the monitor chamber should allow to normalize the current in the 4 test gaps, even without a precise knowledge of the gas temperature and pressure. In Fig. 8 we show the ratio between the currents in the test chambers and the average of the 4 currents in the monitor gaps, as function of time. The ratios are stable within 10% level, proving no evidence of aging.

We notice that this ratio starts increasing when the pressure starts increasing (after $\sim$ 45

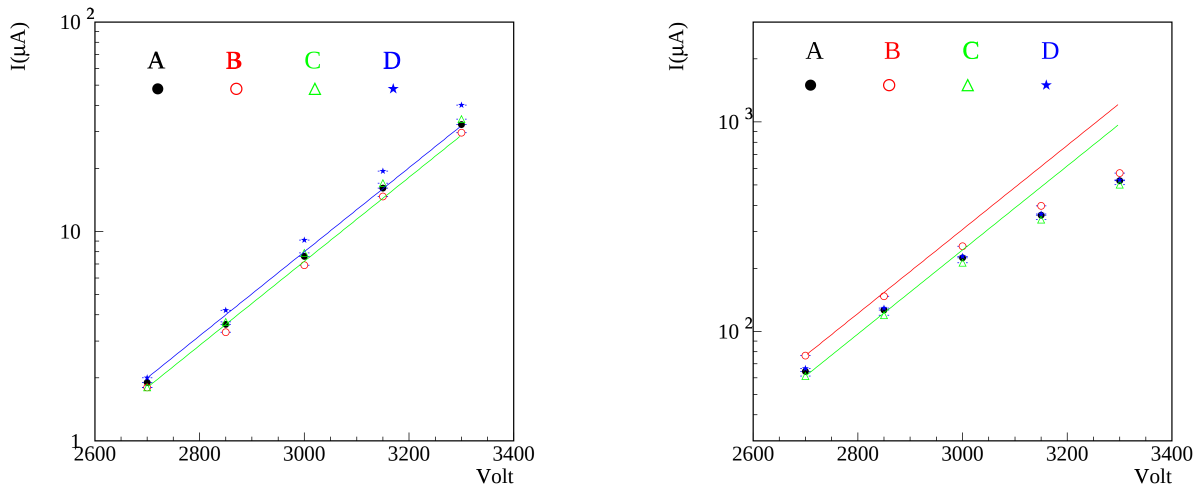

,

Figure 5: Currents in the 4 gaps of the chambers as function of high voltage. LEFT: monitor chamber. The plots show that the gaps were operating in non-saturated condition still at $3300V$: they represent the current at 2700 V extrapolated assuming that for an increase of 150 V, the gas gain doubles (upper line: gap D; lower line: gap C). RIGHT: test chamber. The lines show that the gaps were operating in saturated condition during the aging test at $3300V$ (upper line: gap B; lower line: gap C).

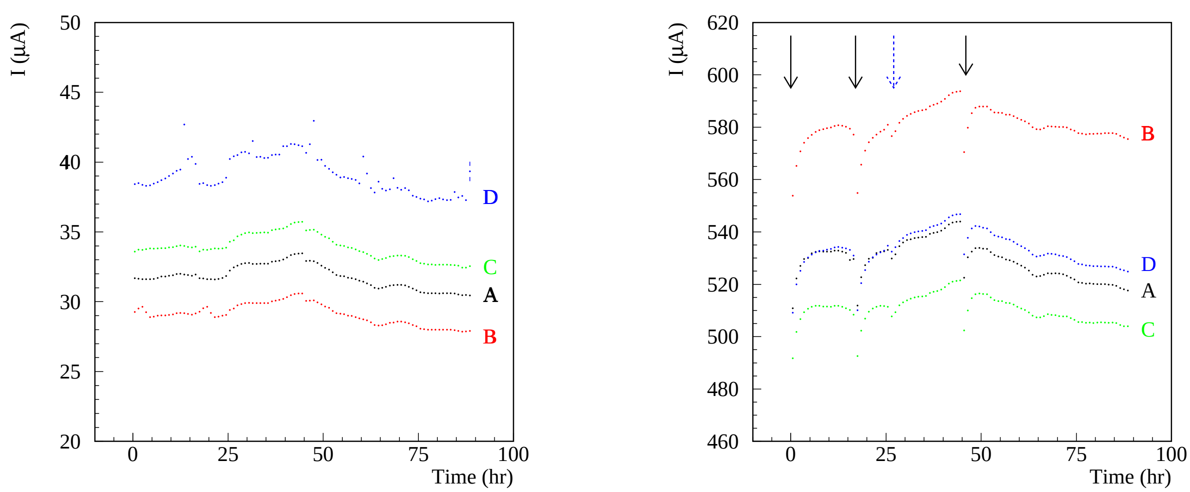

,

Figure 6: Currents in the 4 gaps of the chambers as function of time. LEFT:monitor chamber. RIGHT: test chamber. The smaller values are recorded either just after an access (full arrows) during which the chambers were switched off, or after some measurements at smaller HV (dashed arrow).

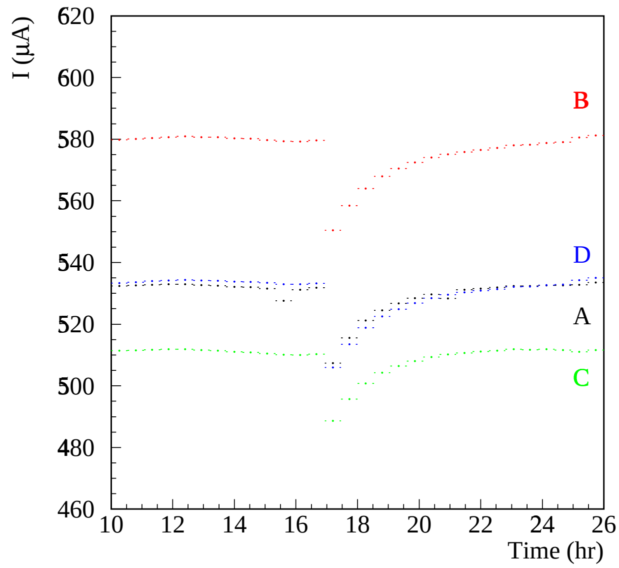

Figure 7: Currents in the 4 gaps of the test chambers as function of time, just before and after an access in the source room. Several hours are needed to reach stable currents.

hours). This is due to the fact that the test gaps are less sensible to pressure variation, because they are operating in a saturated regime. This is shown in Fig. 9 showing the currents (in both chambers) as function of T/P. The parameters of linear fits of $ln(I)\ vs.\ T/P$:

$$ln(I) = \alpha V \cdot T/P + ln(K) \qquad (2)$$

are reported in Table 4. We notice that the slopes are smaller for the test chamber gaps, due to the saturation of gas gain.

MONITOR	ln(K)	Slope	χ^2/NDF	TEST	ln(K)	Slope	χ^2/NDF
A	-1.76	0.0181	97/10	A	3.62	0.00916	32/10
B	-2.06	0.0188	194/10	B	5.10	0.00438	89/10
C	-1.74	0.0182	238/10	C	4.60	0.00568	31/10
D	-2.38	0.0209	204/10	D	4.36	0.00666	49/10
Average	-2.10	0.0194	241/10				

Table 4: Parameters of the linear fit of $ln(I)$ as function of T/P for monitor and test chambers. Last row contains results of the fit of $ln(I_M)$ where I_M is the average current in the 4 monitor gaps.

In Fig. 10 we show the integrated charges as function of time. For the 4 gaps of the test chamber, the integrated charges are in the range $46 \div 54mC/cm$.

In Table 5 (left) we report the integrated charge for 10 equivalent LHC years, for different

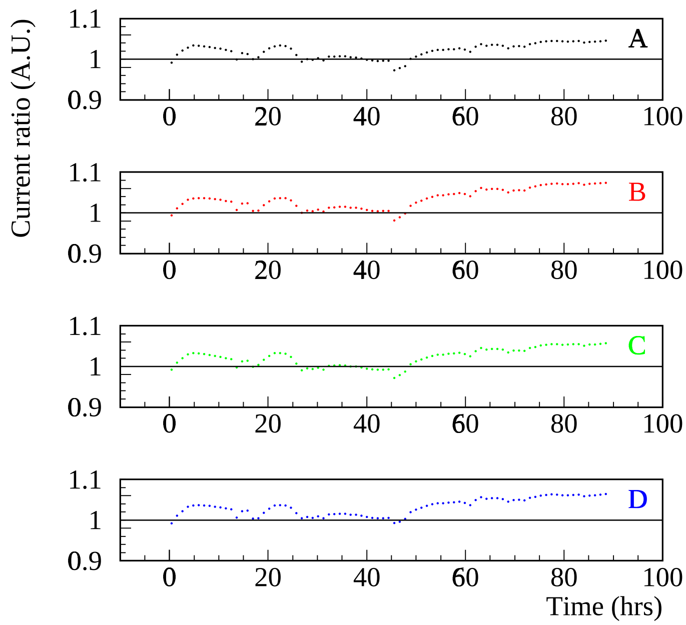

Figure 8: Ratios between the currents in the test chambers and the average of the 4 currents in the monitor gaps, as function of time. The ratios are normalized to their initial values.

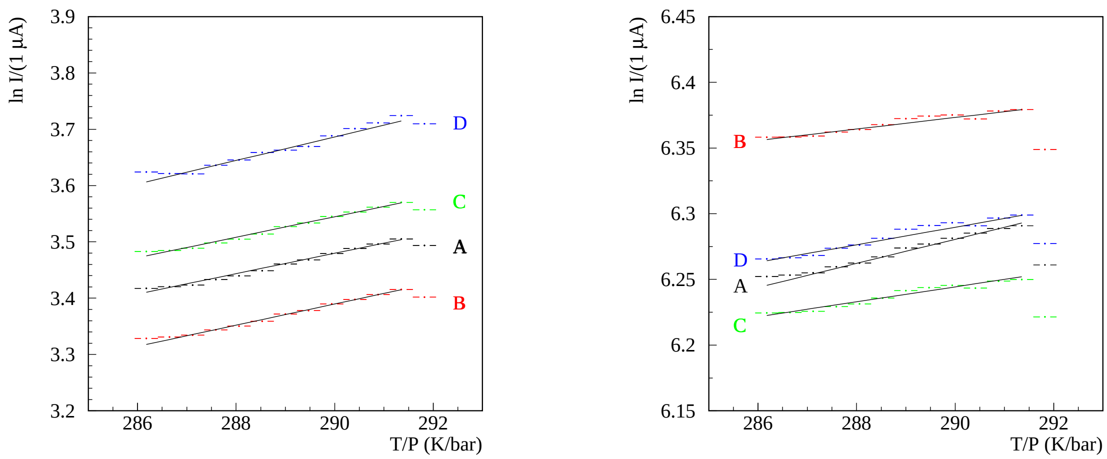

,

Figure 9: Currents in the chambers as function of the ratio of temperature over atmospheric pressure. Straight lines are the best exponential fit results. LEFT: monitor chamber. RIGHT: test chamber.

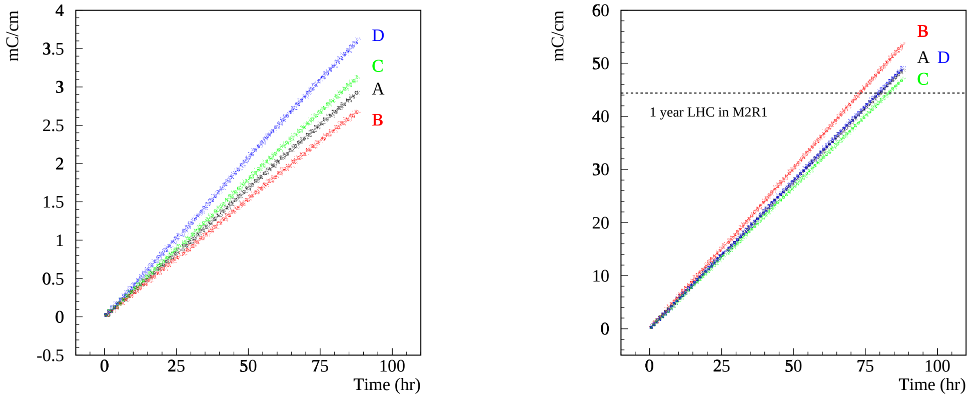

,

Figure 10: Integrated charges as function of time. LEFT: monitor chamber. RIGHT: test chamber.

detector regions, assuming a wire pitch of 1.5 mm, as in the present test. The charges for the tested regions are shown in bold.

	M1	M2	M3	M4	M5
R1	1.214	0.198	**0.053**	0.069	**0.046**
R2	0.491	0.140	**0.017**	**0.023**	**0.019**
R3	0.211	0.069	**0.011**	**0.008**	**0.007**
R4	0.066	**0.013**	**0.004**	**0.003**	**0.002**

	M1	M2	M3	M4	M5
R1	1.62	0.264	0.070	0.092	0.062
R2	0.655	0.187	0.023	0.031	0.025
R3	0.282	0.092	0.014	0.011	0.009
R4	0.088	0.017	0.006	0.004	0.003

Table 5: Integrated charge (C/cm of wire) in 10 LHC equivalent years for each detector region, assuming: luminosity is $2\ 10^{32}$; safety factor is 2 (in M1) and 5 (in M2-M5); charge per hit is Q=0.88 pC/hit (considered to be measured at relativistic rise); the charge is corrected by a factor 0.5 in M1-M2M3R1R2 (assuming the use of a symmetric cathode) and 2 in M2-M5 (due to photons). LEFT: wire pitch is 1.5 mm (as in the present test); RIGHT: wire pitch 2 mm (final chamber design).

4.3 Considerations for a longer test

In Table 5 (right) we report the integrated charge for 10 equivalent LHC years, for different detector regions, assuming a wire pitch of 2 mm, as set in the final design.

We plan to perform a longer aging test with a new chamber prototype with wire pitch of 2 mm. Due to budget limitations, we cannot perform a test longer than one month. The chamber will be exposed at the same dose rate as in the present test (corresponding to $\sim 50\%$ saturation. This will allow us to test all detector regions but M1-R1R2, as shown in Table 6.

However, following Sauli [6]: ”data collected at high current densities tend to be optimistic” and ”space charge gain saturation can set in at high current densities, possibly decreasing the polymerisation efficiency”. So, the aging effect could be underestimated with a saturated detector.

Therefore we plan to expose also an old chamber prototype (with pitch 1.5 mm) at a lower dose rate, operating in linear regime. From Fig. 5 (RIGHT), we see that at 2850 V the test gaps

	M1	M2	M3	M4	M5
R1	**106**	17	4.6	6.0	4.1
R2	**43**	12	1.5	2.0	1.7
R3	18	6.0	0.9	0.7	0.6
R4	5.8	1.1	0.4	0.2	0.2

Table 6: Number of days needed at Casaccia to test 10 equivalent LHC years (at 196 nA/cm with pitch 2 mm, equivalent to 147 nA/cm with pitch 1.5 mm). We assume that efficiency is 90 %. In bold we show the numbers greater than one month.

are not saturated. The corresponding currents are $\sim$ 119 $\div$ 147 μA, about a factor 4 below the 500 μA of the most exposed chamber.

Multiplying by 4 the numbers in Table 6, we find that the prototype operating at lower current $\sim$ 119 $\div$ 147 μA will allow (in one month) to fully test M1-R4, M2-R3R4, M3, M4, M5.

Our last consideration for the long test concerns the gas temperature measurement. We plan to measure the temperature of the gas just out of the chamber. We are looking for radiation hard temperature sensors that can be read through an analog input device interfaced to the LabView ACQ program.

5 Conclusions

The short aging test described in this note allowed us to check the feasibility of a 10 LHC years equivalent test for the M2R1 detector region with the Calliope facility at ENEA-Casaccia.

We have learned from data analysis that a third detector working in non-saturated regime could be of great help and that the measurement of gas temperature could be important for a complete interpretation of data.

Acknowledgements

We thank L. Trasatti and A. Martini who implemented the software for reading the weather station information.

We thank the staff of the Calliope facility (A. Pasquali, F. Zarbo) for the great help in preparing and realizing the test.

References

[1] LHCb-MUON 2001-120, 4 December 2001.

[2] Muon TDR, CERN/LHCC 2001-010, 28 May 2001.

[3] S. Baccaro, A. Festinesi, B. Borgia, “Gamma and neutron irradiation facilities at ENEA-Casaccia Center (Rome)”, Report CERN-CMS/TN, 95-192 (RADH), 1995.

[4] M. Adamo, S. Baccaro, A. Cecilia, A. Cemmi, A. Pasquali, F. Zarbo, “Metodi dosimetrici presso l’impianto di irraggiamento Calliope”, ENEA Technical Report INN/2000/3.

[5] G.Bencivenni et al., NIM A 488 (2002) 493.

[6] F. Sauli, Invited summary talk at the International Workshop on Aging Phenomena in Gaseous Detectors, DESY, Hamburg, October 2-5, 2001. Nucl. Instr. and Meth. in press.